Aggregation, Reaggregation and Degradation of a Trifunctional Thallium(I) Amide Induced by Weak $Tl^{I}\cdots Tl^{I}$ Attraction

Konrad W. Hellmann, Lutz H. Gade,* Roland Fleischer and Thomas Kottke

Dedicated to Professor Mary McPartlin on the occasion of her 65th birthday

Abstract: Metal exchange of the solvated tripodal lithium amide $[H_3CC\{CH_2N(Li{-}solv)SiMe_3\}_3]$ (**1**, solv = ether solvent) with thallium(I) chloride leads to the previously reported pentametallated dimeric thallium amide $[\{H_3CC(CH_2NSiMe_3)_3\}_2(H)Tl_5]$ (**2**) in high yield. That the redox-induced partial demetallation of the amide presumably occurs at an intermediate stage of the metal exchange is inferred from the isolation and structural characterization of the mixed Tl–Li amide $[H_3CC\{CH_3N(Tl){-}SiMe_3\}_3][H_3CC\{CH_2NSiMe_3\}_3(H)(Tl)(Li{-}thf)]\cdot(toluene)$ (**3**), which has a crystal structure closely related to that of **2**. In both cases the central structural motif, defined by weakly attractive $Tl\cdots Tl$ contacts, is a tetrahedral metal array in which a triangular thallium triamide unit is capped by an exposed Tl atom of a second building block. Compound **3** may be converted to **2** by metal exchange with TlCl. The two supramolecular components of **2** reaggregate upon recrystallization in a nonpolar solvent such as pentane to yield the dimeric aggregate of the fully metallated thallium amide $[H_3CC\{CH_2N(Tl){-}SiMe_3\}_3]_2$ (**4**). An X-ray crystallographic study of **4** established the existence of dimeric aggregation through $Tl\cdots Tl$ interactions leading to a more open dimeric form than **2** and **3**, which is interpreted as being due to a structural mismatch of the building blocks. Compound **4** may be thermally degraded by prolonged stirring in toluene at ambient temperature to yield the previously reported mixed-valence $Tl^{I}Tl^{II}$ amide $[H_3CC(CH_2NSiMe_3)_3Tl_2]$ (**5**).

Keywords
aggregations · amides · metal–metal interactions · subvalent compounds · thallium

Introduction

Aggregation of molecular units, defined by attractive metal–metal interactions, to form finite or infinite supramolecular structural motifs in the solid state is one of the most characteristic, though incompletely understood, features in the chemistry of the heavy post-transition metals. The past ten years have witnessed an intense debate as to the nature of the attractions between formally closed-shell metal atoms with d^{10} and $d^{10}s^2$ electronic configurations.[1] While these interactions have been studied extensively in the chemistry of monovalent gold (d^{10})[2] and the divalent heavy Group 14 metals ($d^{10}s^2$),[3] much less is known about the structures which monovalent thallium compounds ($d^{10}s^2$) may adopt.[4]

A theoretical study of the TlH dimer performed at SCF-CI level led to the conclusion that attractive interactions between the molecules through metal–metal contacts are weak, probably less than 20 $kJ\,mol^{-1}$,[5] a situation which has offered support for alternative explanations for the observed aggregates in the solid. A most suggestive picture is that put forward by von Schnering, aptly termed "the umbrella effect", which relates the packing of molecules in the crystal primarily to their shape, thus generating close metal–metal contacts as a *secondary* effect.[6]

In view of the potential ambiguity in the interpretation of the $Tl\cdots Tl$ contacts between mononuclear molecular species due to the weakness of the interaction, the fixation of several Tl centres at close proximity in polynuclear thallium(I) complexes was thought to offer the opportunity of a higher intermolecular metal–metal "connectivity". The effect that the postulated weak attraction has upon the forms of aggregation in the solid (or possibly in solution) might therefore be enhanced. Such a situation is present in the dimeric aggregate of a completely metallated triaminosilane, $[CH_3Si\{N(Tl)tBu\}_3]_2$, reported by Veith et al., which represents a unique structural array in amide chemistry.[7] In contrast to the almost spheroidal cage formed by the lithium analogue, which is based mainly on ionic amido–N–metal interactions, the thallium compound aggregates via metal–metal contacts generating a structure in which the disposition of the six metal atoms may be viewed as defining a pair of edge-sharing tetrahedra.

In a systematic investigation of this type of behaviour using bidentate and tripodal amido ligands we have recently established a variety of novel types of aggregation for Tl^{I}

---

[*] Priv.-Doz. Dr. L. H. Gade, Konrad W. Hellmann, R. Fleischer, Dr. T. Kottke
Institut für Anorganische Chemie der Universität
Am Hubland, D-97074 Würzburg (Germany)
Fax: Int. code +(931)888-4605
e-mail: lutz.gade@mail.uni-wuerzburg.de

0947-6539/97/0311-1801 $ 17.50+.50/0

amides.[8–10] The compounds were synthesized by metal exchange of the respective lithium amides with TlCl in ether solvents. The metal exchange is in competition with another reaction pathway, partial redox disproportionation, which generates Tl^{II} species that either dimerize to give complexed Tl$_2^{4+}$ units[9] or, as radical species, abstract hydrogen atoms from the ether solvent to generate formally "protonated", that is, incompletely metallated, products.[8] An example of such a product of combined metal exchange and redox disproportionation is the pentanuclear species [$\{H_3CC(CH_2NSiMe_3)_3\}_2$-(H)Tl$_5$] (**2**), obtained in high yield from the reaction of [$H_3CC\{CH_2N(Li$-solv$)SiMe_3\}_3$] (**1**, solv. = ether solvent) with TlCl in dioxane, the remarkable solid-state structure of which we reported recently.[9] Out of this first result several important questions arose: 1) At what stage does the redox-induced demetallation occur? 2) Since the two units aggregating in the solid appear to be dissociated in solution, could a change in the conditions of crystallization lead to a redistribution of the molecular components yielding, ultimately, the completely metallated target product [$H_3CC\{CH_2N(Tl)SiMe_3\}_3]_2$? 3) How would the presumed aggregation of the latter in the solid relate to the result obtained by Veith and coworkers?

In this paper we report the results of a study aimed at elucidating the issues raised above and gaining new insight into the possibility of using molecular thallium(I) compounds as building blocks for discrete supramolecular arrays in solid materials.

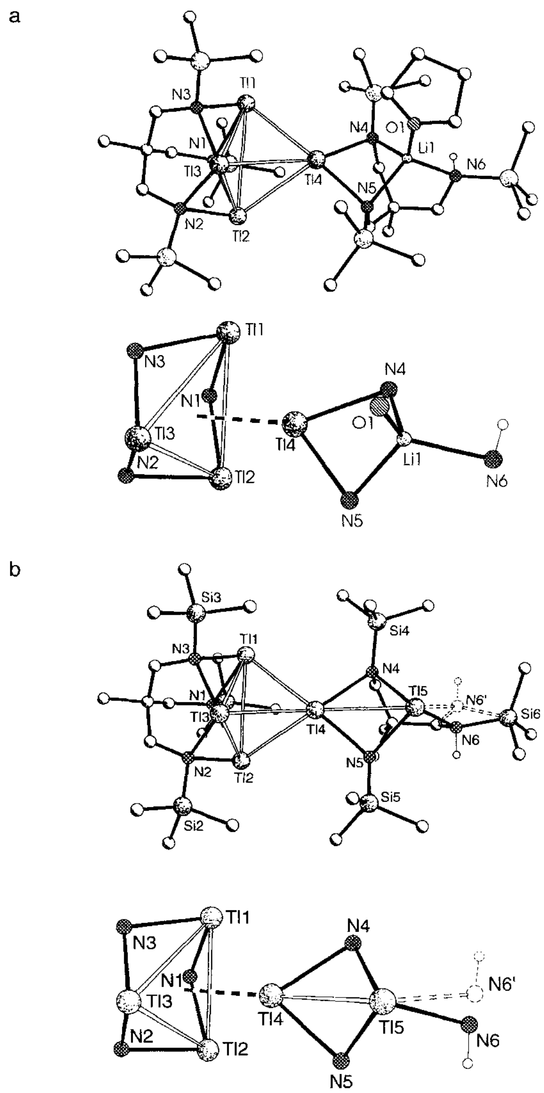

Figure 1. a) Top: molecular structure of **3**; bottom: orientation of the capping Tl unit in **3** with respect to the triangle Tl1-Tl2-Tl3. b) Top: molecular structure of **2**; bottom: orientation of the capping Tl unit in **2** with respect to the triangle Tl1-Tl2-Tl3 (redrawn from ref. [9]).

Results and Discussion

Isolation and Structural Characterization of an Aggregated Mixed Tl–Li–Amide: In order to obtain more detailed information about the course of the metal-exchange reaction between the lithium amide **1** and TlCl to generate **2**, the reaction was carried out in THF, which permits work to be carried out at low temperatures. After addition of TlCl at −30 °C, the cooling bath was removed and the solution stirred for another 10 minutes before the reaction was stopped by removing the solvent in vacuo. After extraction with toluene an orange solution was obtained, from which a mixed Li–Tl amide **3** crystallized in 10–15% yield upon cooling. While the mixed-metallic nature of the amide, its elemental composition and the presence of at least one protonated amido-N function (IR: $\tilde{\nu}$(N–H) = 3390 cm^{-1}) could be deduced from the spectroscopic and analytical data obtained, its correct formulation and structure could only be determined by means of a single-crystal X-ray structure analysis of the compound. This established compound **3** as [$H_3CC\{CH_3N(Tl)SiMe_3\}_3$][$H_3CC\{CH_2NSiMe_3\}_3(H)(Tl)$-(Li–thf)]·(toluene), with a crystal structure which is closely related to the type of cluster arrangement previously determined for **2**. The molecular structure of **3** is depicted in Figure 1 a and the molecular structure of **2** in Figure 1 b.

The relationship between the structures of **2** and **3** is immediately apparent, the most striking feature being in both cases the central tetrahedral arrangement of the thallium atoms. In both cases the amido–N function at N6 is converted to an amino function, as evidenced by the slight pyramidalization of the donor atom [$\sum(\sphericalangle_N) = 348.1°$]. It should be noted that the expected orientation of the lone pair at Tl4 is towards the centre of the metal triangle defined by Tl1–Tl3, as is shown in Figure 1 a (bottom). In the structure of **3** there are three amido-bridged Tl–Tl contacts [Tl1–Tl2 3.8535(7), Tl2–Tl3 3.5180(7), Tl1–Tl3 3.9037(7) Å] and three unsupported metal–metal contacts [Tl1–Tl4 3.3150(6), Tl2–Tl4 3.4611(9), Tl3–Tl4 3.6759(7) Å] which are close to the shortest Tl–Tl distances observed in thallium metal (3.408 and 3.457 Å). As stated previously, we interpret the metal–metal interactions between the Tl centres as being primarily of a van der Waals type, a notion which is supported by the almost complete dissociation in benzene (as determined by cryoscopy), but sufficiently strong to cause the aggregation in the crystalline material. A comparison of the metric parameters related to the Tl$_4$ tetrahedron in **2** and **3** is given in Table 1 b. This establishes the structural array found in the crystal structures of both compounds as an important supramolecular motif in finite aggregates.

The close structural relationship between **2** and **3** raised the question of whether it was possible to convert **3** to **2** by the standard metal-exchange procedure with TlCl. Although some

0947-6539/97/0311-1802 $ 17.50+.50/0

Table 1a. Selected bond lengths [Å] and angles [°] for **3**. Average Tl–N: 2.410 Å, ranging from 2.324(7) (Tl4–N5) to 2.464(8) Å (Tl1–N1).

Tl1–Tl4	3.3150(6)	Tl1–Tl2	3.8535(7)
Tl1–Tl3	3.9037(7)	Tl2–Tl4	3.4611(9)
Tl2–Tl3	3.5180(7)	Tl3–Tl4	3.6759(7)
Tl4-Tl1-Tl2	57.15(2)	Tl4-Tl1-Tl3	60.574(13)
Tl2-Tl1-Tl3	53.935(12)	Tl4-Tl2-Tl3	63.561(13)
Tl4-Tl2-Tl1	53.574(14)	Tl3-Tl2-Tl1	63.761(13)
Tl2-Tl3-Tl4	57.47(2)	Tl2-Tl3-Tl1	62.30(2)
Tl4-Tl3-Tl1	51.765(11)	Tl1-Tl4-Tl2	69.279(14)
Tl1-Tl4-Tl3	67.661(13)	Tl2-Tl4-Tl3	58.974(13)

Table 1b. Comparison of the geometrical features of the central Tl_4 tetrahedra in the previously reported compound **2** as well as in **3**.

	2	**3**
Tl–N av.	2.43	2.410
{min., max.} [Å]	{2.39(1), 2.49(1)}	{2.324(7), 2.464(8)}
Tl–Tl av.	3.590	3.6212
{min., max.} [Å]	{3.403(3), 3.837(3)}	{3.3150(6), 3.9037(7)}
Tl-Tl-Tl av.	61.19	60.00
{min., max.} [°]	{56.07(6), 67.7(7)}	{53.57(1), 69.28(1)}

decomposition is observed upon performing the metal exchange in THF, compound **2** could indeed be isolated from the product mixture in 60–70% yield based on **3** (Scheme 1).

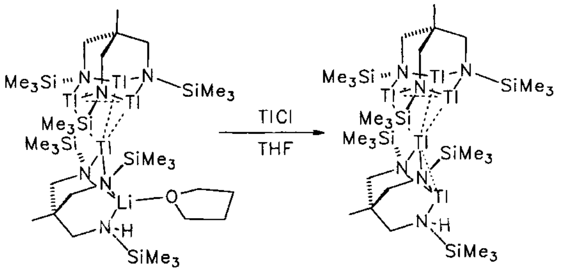

3 **2**

Scheme 1. Conversion of **3** → **2**.

The isolation and characterization of the partially metallated **3** has shown that redox disproportionation inducing partial demetallation of the amides already occurs during the course of the metal-exchange reactions; thus there are two competitive reaction pathways. The demetallation is therefore not the result of a subsequent thermal decomposition of the fully metallated product. This latter aspect will be discussed below in more detail.

Reaggregation of [$H_3CC\{CH_2N(Tl)SiMe_3\}_3$] to Give the Fully Metallated Amido Dimer: As mentioned above, a cryoscopic study of **2** in benzene indicated that the dimeric system is essentially completely dissociated in solution;[9] in other words, in a recrystallization step (performed in toluene) the building blocks of compound **2** first dissociate and then reaggregate, generating the same dimeric arrangement in the solid. The situation described here and the interpretation of **2** as being a weakly bound association of amide building blocks implied that there might be a possibility of obtaining a different combination of the components in **2**, and thus a different product, by changing the conditions of crystallization. This proved to be the case for solvents of reduced polarity, namely saturated hydrocarbons such as pentane or hexane. Recrystallization of the deep red compound **2** in pentane yielded an orange crystalline product, the analytical data of which were consistent with its formulation as the completely metallated amide [$H_3CC\{CH_2N(Tl)SiMe_3\}_3]_n$ (**4**). A redistribution of the components of **2** had thus taken place (Scheme 2). The isolation of **4** simply by recrystallizing **2** indicates that solvent–solute interactions may be as critical as the weakly attractive Tl–Tl contacts in determining the aggregation of the Tl^I amides, a notion which confirms the interpretation of these interactions given earlier in this paper. Attempts to retrieve the second partially metallated component by crystallization from the mother liquor failed owing to its slow thermal decomposition.

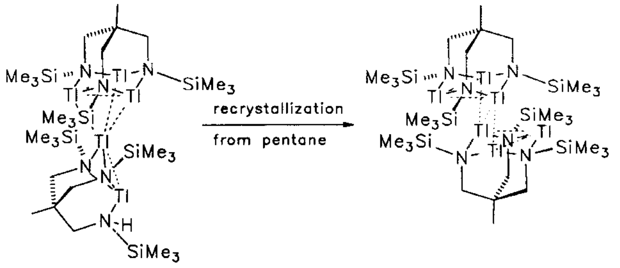

2 **4**

Scheme 2. Isolation of **4** by recrystallization of **2** in pentane.

In order to establish to which degree the molecular amidothallium units in **4** associate in the solid, a single-crystal X-ray structure analysis was carried out. The asymmetric units contains 1.5 dimeric aggregates; the unit cell therefore comprises 3 dimeric units, one of which is generated by the crystallographic centre of inversion. The arrangement of the monomeric subunits within the complete dimer of the asymmetric unit suggests the presence of a second centre of inversion. However, this could not be established crystallographically, as confirmed by applying the Le Page algorithm.[11] Both types of dimers are structurally closely related, and therefore only average metric parameters will be discussed. The dimer that is not located around the centre of inversion is shown in Figure 2, while the principal bond lengths and angles are listed in Table 2.

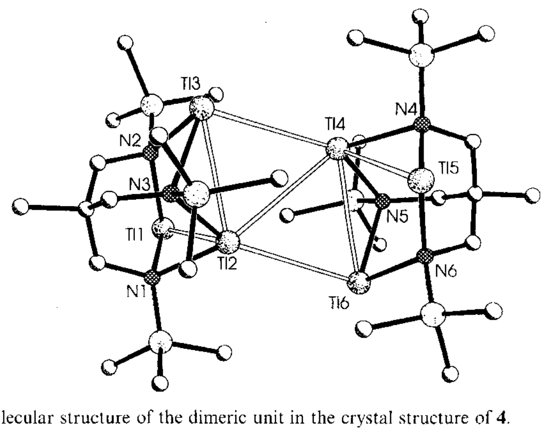

Figure 2. Molecular structure of the dimeric unit in the crystal structure of **4**.

Table 2. Selected bond lengths [Å] and angles [°] for **4**. Average Tl–N: 2.45 Å, ranging from 2.34(2) Å (Tl2–N1) to 2.55(2) Å (Tl1–N2 and Tl3–N1).

Tl1–Tl2	3.519(4)	Tl4–Tl5	3.663(4)
Tl2–Tl3	3.411(3)	Tl7–Tl9	3.643(4)
Tl2–Tl6	3.767(3)	Tl8–Tl9	3.542(3)
Tl2–Tl4	3.768(3)	Tl8–Tl9A	3.706(3)
Tl3–Tl4	3.793(3)	Tl9–Tl9A	3.807(4)
Tl4–Tl6	3.566(3)		
Tl3-Tl2-Tl1	86.09(9)	Tl5-Tl4-Tl3	100.11(8)
Tl3-Tl2-Tl6	120.05(8)	Tl2-Tl4-Tl3	53.63(6)
Tl1-Tl2-Tl6	99.35(8)	Tl4-Tl6-Tl2	61.77(6)
Tl3-Tl2-Tl4	63.55(7)	Tl9-Tl8-Tl9A	63.34(7)
Tl1-Tl2-Tl4	95.86(9)	Tl8-Tl9-Tl7	79.02(8)
Tl6-Tl2-Tl4	56.49(6)	Tl8-Tl9-Tl8A	116.66(7)
Tl2-Tl3-Tl4	62.82(7)	Tl7-Tl9-Tl8A	102.09(8)
Tl6-Tl4-Tl5	77.82(8)	Tl8-Tl9-Tl9A	60.43(7)
Tl6-Tl4-Tl2	61.74(6)	Tl7-Tl9-Tl9A	91.53(9)
Tl5-Tl4-Tl2	89.05(9)	Tl8A-Tl9-Tl9A	56.23(6)
Tl6-Tl4-Tl3	115.37(8)		

The structural centrepiece of the dimeric aggregates is the array of the six Tl atoms joined by amido bridges within the molecular units and by Tl···Tl contacts between the two tripodal amides [d_{av}(Tl–Tl) = 3.768 Å]. In this way an open ladder-type structure of the dimeric units emerges in which each half is distorted considerably with respect to the almost ideally threefold symmetric trithallium units in **2** and **3** which are "capped" by the linking Tl atom (Tl4) in the latter. This appears to imply that in a supramolecular aggregate based on attractive metal–metal interactions the "best fit" through such contacts may be achieved by combination of nonequal, that is, complementary building blocks, generating polyhedral metal arrays with maximum Tl···Tl connectivity. This is not the case in the structure of **4**, in which two Tl atoms (Tl2 and Tl4 in Figure 2) are bent towards each other to come into contact, a situation which is most apparent when the trithallium amido units of **2, 3** and **4** are viewed along an axis defined by the bridgehead C–CH$_3$ axis of the tripodal ligands (Figure 3). Whereas the symmetrically capped Tl$_3$ unit in **2** and **3** displays almost ideal threefold symmetry, one of the Tl atoms in **4**, Tl2, protrudes out of the plane otherwise spanned by the metal atoms of the monomeric unit in **4**, pushing the other two Tl atoms Tl1 and Tl3 further apart (4.61 Å).

A closer inspection of the way these dimeric units are packed in the crystal reveals no significant intermolecular metal–metal interactions, the shortest Tl–Tl distance being larger than 4.3 Å and thus outside the range of significant intermolecular contacts. Figure 4a displays the relative arrangement of two dimeric units, while a view of the unit cell of **4** is offered in Figure 4b.

A comparison of the crystal structure of Veith's [H$_3$CSi{N(Tl)*t*Bu}$_3$]$_2$ with that established for compound **4** is instructive. In both cases an aggregation through Tl···Tl contacts is observed with the two (distorted) Tl$_3$ triangles adopting a "slipped" arrangement with respect to each other. However, **4** aggreggates to form a more open Tl$_6$ array, possibly as a consequence of the greater degree of steric demand of the ligand periphery operating in the latter.

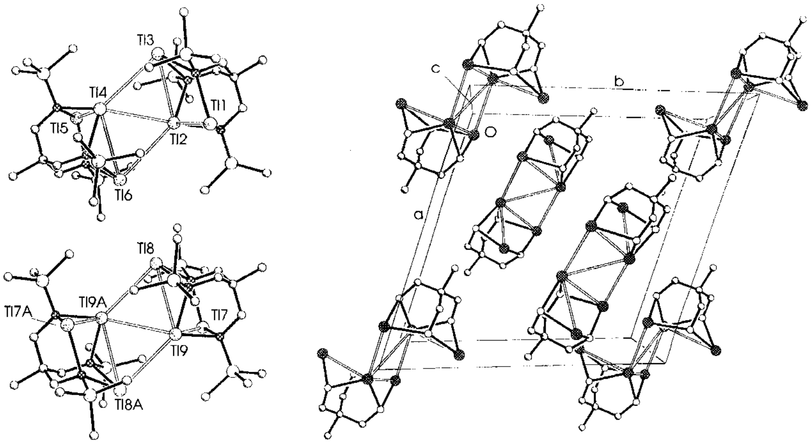

Figure 4. Packing of the dimers in the crystal structure of **4**. The SiMe$_3$ groups of the amide units are not shown in the view of the unit cell for reasons of clarity.

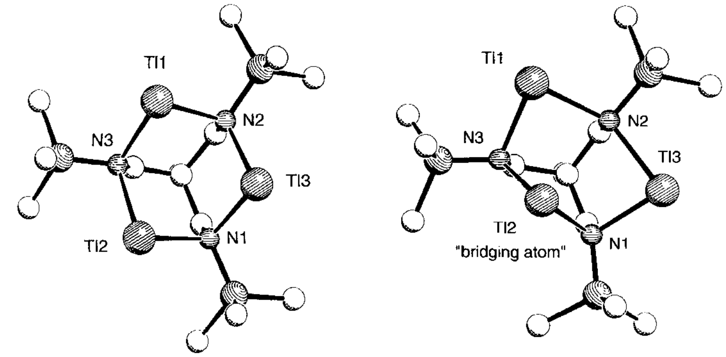

Figure 3. Comparison of the Tl$_3$ building blocks in **2** and **3** (a) and in **4** (b) showing the distortion of the latter from the almost trigonal symmetry found for the centrally "capped" Tl$_3$ triangles.

Redox Disproportionation of [H$_3$CC{CH$_2$N(Tl)SiMe$_3$}$_3$]$_2$ (4): While compound **4** appears to be stable in pentane solution over a period of several days or weeks, its solution in toluene undergoes selective redox disproportionation to yield thallium metal and the previously reported Tl^{I}Tl^{II} mixed-metal species [H$_3$CC(CH$_2$NSiMe$_3$)$_3$Tl$_2$]$_2$ (**5**), which was shown to contain a covalent Tl^{II}–Tl^{II} bond (Scheme 3).[9] After the solution had been stirred at ambient temperature for 24 hours complete conversion had occurred and the product could be isolated simply by centrifugation of the metallic thallium, separation of the solution and removal of the solvent. We have previously reported the isolation of this compound in ca. 30% yield after stirring the lithium amide **1** and thallium chloride for three days and subsequent work-up. The selective generation of **5** from the completely metallated species **4** sheds new light upon the way this mixed-valence compound is generated. We now propose that in the course of the metal exchange of the Li amide with TlCl, redox disproportionation of partially transformed mixed-metal species leads to radical intermediates that abstract the hydrogen atoms from the ether solvents, forming incompletely

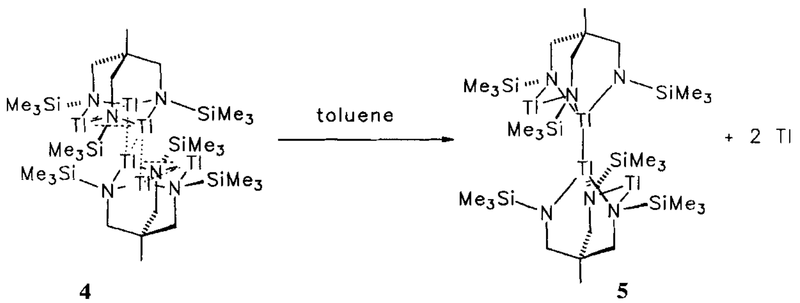

4 **5**

Scheme 3. Selective thermal redox disproportionation of **2** in toluene to yield the previously characterized mixed-valence species **5**.

metallated species such as **2** and **3**, whereas the slower redox degradation of the fully transmetallated compound **4** affords the dimeric Tl^ITl^{II} complex, which is characterized by the covalent Tl–Tl bond. The partially "protonated" molecular fragments observed appear to decompose thermally with concomitant precipitation of Tl metal, while complex **5** is considerably more stable and may be isolated even after prolonged stirring in solution. The proposal put forward is additionally supported by the isolation of **5** from solutions of **2** and **3** in quantities accounting for the amount of $[H_3CC\{CH_2N(Tl)SiMe_3\}_3]$. The network of reactions proposed here is summarized in Scheme 4.

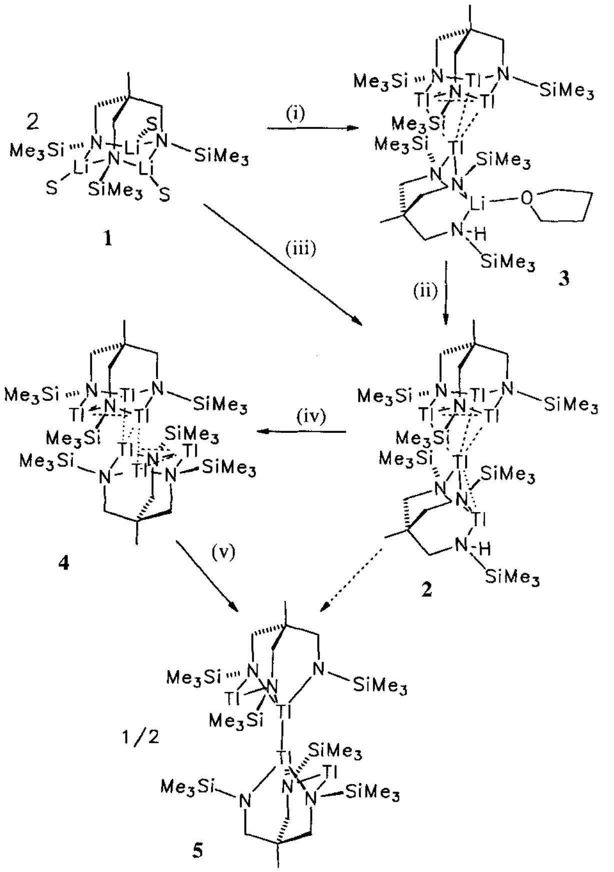

Scheme 4. Summary of the conversions of the tripodal amides (S = ether). i) TlCl/THF, 10 min; ii) TlCl/THF 3 h; iii) TlCl/dioxane; iv) recrystallization from pentane; v) thermal degradation in toluene

Conclusions

Thallium amides of the type discussed in this paper aggregate in solids to generate finite or infinite supramolecular structural motifs defined by weak metal–metal contacts. The monomeric units may be viewed as building blocks which, depending upon the conditions of crystallization, may form different aggregates as established by the redistribution of compound **2** to yield **4**. Redox disproportionation is a prevalent feature of this type of chemistry and may lead to partial demetallation of the amides or the formation of well-defined mixed-valent species. The reaction pathways leading to either of the two products appear to depend on the stage in the synthesis of the Tl^I amides at which the redox chemical degradation takes place.

In current and future studies we are investigating the possibility of combining different Tl^I building blocks having complementary "sticky ends". These should be able to form discrete polyhedral arrays of maximum metal–metal connectivity such as the tetrahedra that are characteristic of the solid-state structures of **2** and **3**.

Experimental Procedure

All manipulations were performed under purified argon in standard (Schlenk) glassware, which was flame-dried with a Bunsen burner prior to use. Solids were separated from suspensions by centrifugation only, all filtration procedures being thus avoided. The centrifuge employed was a Rotina 48 (Hettich, Tuttlingen, Germany), which was equipped with a specially designed Schlenk tube rotor.[12] Solvents were dried according to standard procedures. The deuterated solvents used for the NMR spectroscopic measurements were degassed by three successive "freeze-pump-thaw" cycles and dried over 4 Å molecular sieves. All other chemicals were used as previously reported.[9, 13, 14]

The ^1H and ^7Li NMR spectra were recorded on a Bruker AC 200 spectrometer equipped with a B-VT-2000 variable-temperature unit (200.13 and 77.78 MHz, respectively) with tetramethylsilane and LiI (1 M in H_2O, ext.) as references. Attempts to record ^{13}C NMR spectra were unsuccessful owing to considerable decomposition of the samples in the course of the experiments. Elemental analyses were carried out in the microanalytical laboratory of the chemistry department at Würzburg.

Preparation of $[\{H_3CC(CH_2NSiMe_3)_3\}_2(H)(Li\text{–}thf)Tl_4]\cdot(CH_3C_6H_5)$ (3): TlCl (2.16 g, 9.00 mmol) was added to a stirred solution of $[H_3CC\{CH_2N(Li)SiMe_3)_3\}(thf)_3]$ (1.70 g, 3.00 mmol) in THF (30 mL) at −30 °C. After the mixture had been stirred for 10 min at room temperature the solvent was removed in vacuo and the residue extracted with toluene (20 mL). The mixture was centrifuged and the isolated red solution concentrated to ca. 8 mL. After storage at −35 °C for several days, compound **3** was obtained as an orange crystalline solid (toluene monosolvate). Yield 0.52 g, 0.32 mmol (21 %). ^1H NMR (200.13 MHz, $[D_6]$benzene, 25 °C): $\delta = 0.17$ (s, 27 H; $Si(CH_3)_3$), 0.25 (s, 27 H; $Si(CH_3)_3$), 0.56 (s, 3 H; H_3CC), 0.66 (s, 3 H; H_3CC), 1.29 (m, 4 H; CH_2CH_2O), 2.10 (s, 3 H; $C_6H_4CH_3$), 2.95–3.38 (br m, 12 H; $C(CH_2)_3$), 3.53 (m, 4 H; CH_2CH_2O), 6.95–7.14 (m, 5 H; $C_6H_4CH_3$); $\{^1H\}^7Li$ NMR (77.78 MHz, $[D_6]$benzene, 25 °C, LiI/H_2O): $\delta = 4.20$; $C_{39}H_{88}LiN_6OSi_6Tl_4$ (1650.15): calcd C 28.37, H 5.43, N 5.09, Tl 49.51; found C 28.01, H 5.23, N 4.85, Tl 49.31.

Preparation of $[H_3CC\{CH_2N(Tl)SiMe_3\}_3]_2$ (4): $[\{H_3CC(CH_2NSiMe_3)_3\}_2(H)Tl_5]$ (**2**, 1.00 g, 0.59 mmol) was dissolved at room temperature in pentane (25 mL). The red solution was concentrated to ca. 15 mL and compound **4** precipitated as an orange crystalline solid after storage at −35 °C for 12 h. Yield based on the fully metallated fragment in **2**: 0.41 g, 0.22 mmol (73 %). ^1H NMR (200.13 MHz, $[D_6]$benzene, 25 °C): $\delta = 0.21$ (s, 54 H; $Si(CH_3)_3$), 0.55 (s, 6H; H_3CC), 3.52 (brs, 12H; $C(CH_2)_3$); $C_{28}H_{72}N_6Si_6Tl_6$ (1887.73) calcd C: 17.82, H 3.84, N 4.45, Tl 64.96; found C 17.01, H 3.63, N 4.25, Tl 64.61.

Conversion of 3 to $[\{H_3CC(CH_2NSiMe_3)_3\}_2(H)Tl_5]$ (2): TlCl (14.5 mg, 0.06 mmol) was added to a stirred solution of $[\{H_3CC(CH_2NSiMe_3)_3\}_2(H)(Li{-}thf)Tl_4]\cdot(C_7H_7)$ (100 mg, 0.06 mmol) in THF (10 mL) at −30 °C. After the mixture had been stirred for 25 min at room temperature the solvent was removed in vacuo and the residue extracted with 10 mL toluene. The mixture was centrifuged and the isolated red solution concentrated to ca. 4 mL. Compound **2** (67 mg, 0.042 mmol) crystallized at −35 °C as a red solid in 69% yield. The analytical, crystallographic and spectroscopic properties of the isolated material were identical to those reported previously for **2**.[9]

Conversion of 4 to $[H_3CC(CH_2NSiMe_3)_3Tl_2]_2$ (5): Solid **4** (100 mg, 0.05 mmol) was dissolved in toluene (10 mL) and stirred at room temperature for 24 h. During this period thallium metal precipitated as a grey-black powder. After centrifugation the solvent was removed in vacuo. The ^1H NMR spectrum of the product indicated almost complete conversion of **4** to **5**. An analytically pure sample was obtained after the centrifugation by concentrating the supernatant yellow solution to ca. 3 mL and storing the solution at −35 °C. The yellow, crystalline solid had identical analytical, spectroscopic and crystallographic properties to those reported previously for **5**.[9]

X-ray Crystallographic Study of 3 and 4: Data for **3** were collected at −120 °C from an oil-coated shock-cooled crystal[15] on a Stoe-Siemens AED using $Mo_{K\alpha}$ radiation (λ = 0.71073 Å). Intensity data were measured with profile-fitted[16] $2\theta/\omega$ scans. Semiempirical absorption correction was applied using azimuthal (ψ-) scans ($\psi > 80°$).[17] Crystals of **4** were selected and mounted at −50 °C in a drop of perfluorinated polyether using a low-temperature crystal mounting device. Data were collected at −100 °C with profile-fitted ω scans on an Enraf–Nonius CAD4 four-circle diffractometer equipped with a homemade low-temperature device and using graphite-monochromated $Mo_{K\alpha}$ radiation (λ = 0.71073 Å). Semiempirical absorbtion correction was performed using azimuthal (ψ-) scans ($\psi > 80°$). Both structures were solved by Patterson methods (SHELXS-90[18a]) and refined to convergence by full-matrix, least-squares iteration against F^2 (SHELXL-96[18b]) minimizing the function $w(F_o^2 - F_c^2)$ where $w = 1/[\sigma^2(F_o^2) + (g_1P)^2 + g_2P]$ and $P = [\max(F_o^2,0) + 2F_c^2]/3$. Unless otherwise stated, non-hydrogen atoms were refined anisotropically using geometric and ADP restraints. A riding model was employed in the refinement of the hydrogen atom positions, with the isotropic displacement parameters fixed to 1.2 times (NH, CH, CH_2) and 1.5 times (CH_3) the value of U_{eq} of the attached carbon atom. The carbon atoms of the $SiMe_3$ groups in **4** were refined with equal isotropic U values within each group; geometric restraints were applied. The crystallographic data of both structures are reported in Table 3.

Crystallographic data (excluding structure factors) for the structures reported in this paper have been deposited with the Cambridge Crystallographic Data Centre as supplementary publication no. CCDC-100594. Copies of the data can be obtained free of charge on application to The Director, CCDC, 12 Union Road, Cambridge CB2 1EZ, UK (Fax: Int. code +(1223)336-033; e-mail: deposit@chemcrys.cam.ac.uk).

Acknowledgements: This work was supported by the Deutsche Forschungsgemeinschaft (Schwerpunktprogramm "Polyeder"). We thank Professor D. Stalke for stimulating discussions and Professor H. Werner for his continued interest and support.

Received: April 23, 1997 [F 674]

Table 3. Crystallographic data for **3** and **4**.

	3	**4**
empirical formula	$C_{39}H_{89}LiN_6OSi_6Tl_4$	$C_{14}H_{36}N_3Si_3Tl_3$
M_r	1651.12	943.84
T, K	153(2)	173(2)
space group	$P\bar{1}$	$P\bar{1}$
a, Å	11.2294(14)	15.090(8)
b, Å	14.582(3)	15.245(9)
c, Å	19.861(3)	18.039(12)
α, °	69.467(6)	101.35(6)
β, °	89.529(8)	99.11(4)
γ, °	74.458(9)	105.5(5)
cell volume, Å^3	2920.8(8)	3822(4)
Z	2	6
ρ_{calcd}, Mg m^{-3}	1.877	2.461
absorption coeff, mm^{-1}	11.155	19.071
$F(000)$	1568	2556
crystal size, mm^3	0.40 × 0.30 × 0.30	0.15 × 0.15 × 0.10
θ range	$4.04 \leq \theta \leq 22.56$	$3.03 \leq \theta \leq 22.48$
reflections collected	8053	11967
independent reflections	7655 [R(int) = 0.0530]	9942 [R(int) = 0.0998]
absorption correction	semiempirical (ψ-scans)	semiempirical (ψ-scans)
max. and min. transmission	0.1074 and 0.0687	0.3130 and 0.1888
data/restraints/parameters	7655/275/536	9942/874/469
GoF on F^2	1.041	0.980
final R indices [$I > 2\sigma(I)$]	$R(F)$ = 0.0352 [a]	$R(F)$ = 0.0870 [a]
(all data)	$wR(F^2)$ = 0.0847 [b]	$wR(F^2)$ = 0.2169 [b]
Extinction coefficient	0.00073(6)	n/a
largest diff peak and hole, e Å^{-3}	1.754 and −1.266	2.198 and −3.109
g_1, g_2	0.0444, 10.5953	0.0469, 1.5516

[a] $R(F) = \sum||F_o| - |F_c||/\sum|F_o|$. [b] $wR(F^2) = [\sum[w(F_o^2 - F_c^2)^2]/\sum[w(F_o^2)^2]]^{1/2}$.

---

[1] *Unkonventionelle Wechselwirkungen in der Chemie metallischer Elemente* (Ed.: B. Krebs), VCH, Weinheim, **1992**.

[2] d^{10}–d^{10} interactions in Ag^I and Au^I compounds, see for example: a) A. Dedieu, R. Hoffmann, *J. Am. Chem. Soc.* **1978**, *100*, 2074; b) P. Pyykkö, Y.-F. Zhao, *Angew. Chem.* **1991**, *103*, 622; *Angew. Chem. Int. Ed. Engl.* **1991**, *30*, 604; c) H. Schmidbaur, *Gold Bull.* **1990**, *23*, 11; d) H. Schmidbaur, *Chem. Soc. Rev.* **1995**, *24*, 391; e) D. M. P. Mingos, *J. Chem. Soc. Dalton Trans.* **1996**, 561; f) M. Jansen, *Angew. Chem.* **1987**, *99*, 1136; *Angew. Chem. Int. Ed. Engl.* **1987**, *26*, 1098; g) N. Kaltsoyannis, *J. Chem. Soc. Dalton Trans* **1997**, 1.

[3] M. Veith, *Chem. Rev.* **1990**, *90*, 3.

[4] Theoretical work: a) C. Janiak, R. Hoffmann, *Angew. Chem.* **1989**, *101*, 1706; *Angew. Chem. Int. Ed. Engl.* **1989**, *28*, 1688; b) C. Janiak, R. Hoffmann, *J. Am. Chem. Soc.* **1990**, *112*, 5024. c) C. Janiak, R. Hoffmann in ref. [1], p. 45; d) G. Treboux, J.-C. Barthelat, *J. Am. Chem. Soc.* **1993**, *115*, 4870. Selected examples of structurally characterized Tl^I compounds: e) H. Schumann, C. Janiak, J. Pickart, U. Börner, *Angew. Chem.* **1987**, *99*, 788; *Angew. Chem. Int. Ed. Engl.* **1987**, *26*, 789; f) J. S. Casas, A. Castineiras, I. Haiduc, A. Sanchez, J. Sordo, E. M. Vasques-Lopez, *Polyhedron* **1994**, *13*, 1805; g) H. Pritzkow, P. Jennische, *Acta Chem. Scand.* **1975**, *A29*, 60; h) R. Atencio, J. Barbera, C. Cativiela, F. J. Lahoz, J. L. Serrano, M. M. Zurbano, *J. Am. Chem. Soc.* **1994**, *116*, 11558; i) P. Jutzi, D. Wegener, M. B. Hursthouse, *Chem. Ber.* **1991**, *124*, 1660; j) P. Jutzi, J. Schnittger, M. B. Hursthouse, *ibid.* **1991**, *124*, 4870; k) D. Labahn, E. Pohl, R. Herbst-Irmer, D. Stalke, H. W. Roesky, G. M. Sheldrick, *ibid.* **1991**, *124*, 1127; l) S. D. Waezsada, T. Belgardt, M. Noltemeyer, H. W. Roesky, *Angew. Chem.* **1994**, *106*, 1413; *Angew. Chem. Int. Ed. Engl.* **1994**, *33*, 1351; m) K. W. Klinkhammer, S. Henkel, *J. Organomet. Chem.* **1994**, *480*, 167; n) W. Uhl, S. U. Keimling, K. W. Klinkhammer, W. Schwarz, *Angew. Chem.* **1997**, *109*, 64; *Angew. Chem. Int. Ed. Engl.* **1997**, *36*, 64.

[5] P. Schwerdtfeger, *Inorg. Chem.* **1991**, *30*, 1660.

[6] Cited in ref. [4b] (as personal communication, ref. [132]).

[7] M. Veith, A. Spaniol, J. Pöhlmann, F. Gross, V. Huch, *Chem. Ber.* **1993**, *126*, 2625.

[8] K. W. Hellmann, L. H. Gade, I. J. Scowen, M. McPartlin, *Chem. Commun.* **1996**, 2515.

[9] K. W. Hellmann, L. H. Gade, A. Steiner, D. Stalke, F. Möller, *Angew. Chem.* **1997**, *109*, 99; *Angew. Chem. Int. Ed. Engl.* **1997**, *36*, 160.

[10] K. W. Hellmann, L. H. Gade, R. Fleischer, D. Stalke, *Chem. Commun.* **1997**, 527.

[11] Y. Le Page, *J. Appl. Crystallogr.* **1982**, *15*, 255.

[12] K. W. Hellmann, L. H. Gade, *Verfahrenstechnik*, **1997**, *31 (5)*, 70.

[13] L. H. Gade, N. Mahr, *J. Chem. Soc. Dalton Trans.* **1993**, 489.

[14] K. W. Hellmann, L. H. Gade, W.-S. Li, M. McPartlin, *Inorg. Chem.* **1994**, *33*, 5974.

[15] a) T. Kottke, D. Stalke, *J. Appl. Crystallogr.* **1993**, *26*, 615; b) T. Kottke, R. J. Lagow, D. Stalke, *ibid.* **1996**, *29*, 465.

[16] W. Clegg, *Acta Crystallogr. A* **1981**, *37*, 22.

[17] A. C. T. North, D. C. Phillips, F. S. Mathews, *Acta Crystallogr. A* **1968**, *24*, 351.

[18] a) G. M. Sheldrick, *Acta Crystallogr. A* **1990**, *46*, 467; b) G. M. Sheldrick, **1996** version of *SHELXL-93, Program for crystal structure refinement*, Göttingen, **1993**.